# SURFACE AREA AND LAYER CHARGE OF SMECTITE FROM CEC AND EGME/H₂O-RETENTION MEASUREMENTS

JAN ŚRODOŃ[1] AND DOUGLAS K. MCCARTY[2]

[1] Institute of Geological Sciences PAN, Senacka 1, 31002 Krakow, Poland
[2] Chevron ETC, 3901 Briarpark, Houston, TX 77042, USA

**Abstract**—The total specific surface area (*TSSA*) and smectitic layer charge ($Q_s$) calculated from the structural formulae and unit-cell dimensions of 12 pure smectite samples were used as a reference in the design and evaluation of *TSSA* and $Q_s$ measurement techniques based on cation exchange capacity (*CEC*), H₂O retention at 47% RH, and ethylene glycol monoethyl ether (EGME) retention. A thermogravimetric analysis-mass spectrometry (TGA-MS) technique was used to study the release of H₂O from smectite on heating, and to introduce a correction for H₂O remaining in the smectite after heating to 110ºC, because the sample weight at this temperature has been used routinely as a reference in *CEC* and EGME sorption measurements. A temperature of 200ºC was found to be the optimum reference for such measurements.

A good agreement between $Q_s$ from the structural formula and from *CEC* was obtained when this correction was applied. The *TSSA* of smectite was measured with similar accuracy (mean error of ±5−7%) by three techniques: (1) using mean H₂O coverage; (2) using mean EGME coverage; and (3) using a combination of H₂O coverage and *CEC*. A reduction of the mean error from 5−7% to 4% can be obtained by averaging these measurements, and a further reduction to 3% by introducing corrections for the dependence of H₂O and EGME coverage on layer charge. The study demonstrates that Ca²⁺-smectite samples at 47% RH have H₂O contents corresponding to 88−107% of the theoretical mass of a monolayer and offers an explanation of this variation.

**Key Words**—*CEC*, Charge Density, EGME, Layer Charge, Smectite, Specific Surface Area, Water Sorption.

## INTRODUCTION

The total specific surface area (*TSSA*, m²/g) of a rock is the maximum area accessible to H₂O molecules, exchangeable cations, and polar molecules dissolved in pore water, *i.e.* the specific surface area, which includes internal surfaces of minerals (Michot and Villieras, 2006, p. 969). The cation exchange capacity (*CEC*, meq/100 g) is the sum of the exchange cations held on the *TSSA* of the rock. The ratio of these two parameters is the smectitic surface charge density, which in this paper is expressed as smectitic layer charge, in units of charge per formula unit (O₁₀(OH)₂), and marked as $Q_s$ following Środoń *et al.* (1992). Thus, all three parameters are interrelated, and together they characterize the surface properties of the rock and control or influence the amount of H₂O bound to mineral surfaces, the electrical conductivity of the mineral matrix, the mechanical properties of the rock such as plasticity and swelling, and sorption properties. These properties are all important for numerous industrial applications.

In common sedimentary rocks, *TSSA* and *CEC* are controlled almost exclusively by the presence of finely dispersed layer silicates with charged, smectite-type surfaces that include: smectite, mixed-layer illite-smec-

tite, and illite. Other high-surface rock components like zeolites, vermiculite, kaolinite-smectite, or opal are less abundant. Thus, understanding the *TSSA*-*CEC*-$Q_s$ relationships for smectite is the key to understanding and predicting the physical and mechanical properties of sedimentary rocks.

The *TSSA* of layer silicates can be calculated from geometrical considerations (*TSSA*$_{Nr}$ is used here to represent the theoretical *TSSA*), by approximating the shape of the silicate fundamental particle (Nadeau *et al.*, 1984), *i.e.* a set of *N* permanently bound 2:1 layers between two neighboring expandable interlayers, as a flat cylinder (Środoń *et al.*, 1992):

$$TSSA_{Nr} = \frac{\text{area}}{\text{mass}} = \frac{2\pi r \times Nt_s + 2\pi r^2}{\pi \times r^2 \times Nt_s \times d_s}$$

thus

$$TSSA_{Nr} = \frac{2000}{d_s} \times \left(\frac{1}{Nt_s} + \frac{1}{r}\right) \qquad (1)$$

where *r* is the mean radius of the silicate fundamental particle, $t_s$ is the thickness of an individual silicate layer (both in nm), and $d_s$ is the dry density of smectite layers (g/cm³). In pure smectite, all interlayers are expandable, thus *N* = 1. For this reason *TSSA*$_{Nr}$ of smectite can be calculated precisely. The availability of this calculation made smectite a reference material for all adsorption-

* E-mail address of corresponding author:
ndsrodon@cyf-kr.edu.pl

155

based *TSSA* measurement methods, which are indispensable when the material is not pure smectite.

Direct *TSSA* measurement techniques employ the sorption of different polar molecules on the rock surface, in an attempt to achieve the conditions of monomolecular coverage. The two most popular techniques use ethylene glycol monoethyl ether (EGME) (Carter *et al.*, 1965; Tiller and Smith, 1990) and $H_2O$ (Newman, 1983). The EGME has replaced ethylene glycol used in earlier studies, following Dyal and Hendricks (1950). Several other techniques based on other sorbents, *e.g.* p-nitrophenol (Ristori *et al.*, 1989; Theng *et al.*, 1999) or polyvinylpyrrolidone (PVP) (Blum and Eberl, 2004), have been proposed. In all these methods, *TSSA* is calculated from the measured mass of the adsorbent (mg per 1 g of dry sample), divided by the coverage of 1 $m^2$ by this adsorbent (mg of absorbent per 1 $m^2$ of clay mineral surface), established from a standard with known *TSSA* (typically a smectite). An error inherent to these techniques, well recognized by several studies (*e.g.* Chiou and Rutherford, 1997), comes from the dependence of the adsorbed mass not only on *TSSA* but also on the clay layer charge and partial pressure of the absorbed molecules.

The layer charge of smectites can be obtained directly from the structural formula calculation, if all the interlayer cations in smectite are assigned as exchangeable. The layer charge and its distribution can be measured directly by the alkylammonium technique of Lagaly and Weiss (1969), which takes advantage of the dependence of alkylammonium cation orientation in the smectite interlayer on the layer charge. The molecule orientation is measured from the smectite $d_{001}$ spacing in the XRD pattern of an oriented preparation. It has been well established, though not explained satisfactorily, that $Q_s$ values obtained from smectite structural formulae are systematically greater than those measured by the alkylammonium method (Kaufhold, 2005). Other techniques based on the dependence of smectite $d_{001}$ on the layer charge have been proposed, but they are only semiquantitative (Emmerich and Wolters, 2005).

The *CEC* of smectite is measured by numerous techniques, all employing a selected reagent in order to exchange all the cations occurring naturally in the clay. The *CEC* can be evaluated by measuring the concentrations of the exchanged cations in solution, the concentration of the cation introduced into exchange positions of the clay, or the difference in concentration of the reagent before and after the exchange reaction. This last approach, originally only semi-quantitative, *e.g.* using the methylene blue technique (see Avena *et al.*, 2001), is gaining popularity because it is less labor-intensive and insensitive to the presence of carbonates. More accurate measurement techniques have been developed such as Ag thiourea (Chabra *et al.*, 1975; Dohrmann and Echle, 1994), Co-hexamine (Orsini and Remy, 1976; Bardon *et al.*, 1983; Ciesielski and Steckerman, 1997), and Cu-

amines (Bergaya and Vayer, 1997; Meier and Kahr, 1999; Ammann *et al.*, 2005).

In our opinion, one aspect of the TSSA-*CEC*-$Q_s$ studies that remains underestimated is the weight basis for such measurements. Layer charge, $Q_s$, and $TSSA_{Nr}$ obtained from the structural formula are from an absolutely dry (ignited at 1000−1100ºC) basis, while *TSSA* and *CEC* are routinely measured after the sample is dried for several hours at 110ºC, cooled in a desiccator, and then weighed. Values measured in such different ways are not directly comparable. This study was undertaken in order to investigate the amount of $H_2O$ held by smectite at different temperatures, and to take this factor into account when investigating the *TSSA*-*CEC*-$Q_s$ relationship.

## MATERIALS AND METHODS

### Smectite separation, chemical composition, and XRD characteristics

A set of 12 smectite samples, covering the full range of known smectite layer charge of 0.3−0.6 eq/$O_{10}(OH)_2$ according to the AIPEA classification of layer silicates (*e.g.* Moore and Reynolds, 1997), was selected for this study (Table 1). The smectite compositions included montmorillonite, nontronite, saponite, and hectorite. Beidellite (SBld-1 from The Clay Minerals Society Source Clays Repository) was also inspected but found to be contaminated by kaolinite and kaolinite-smectite even in the <0.2 µm fraction.

All bulk samples were treated to remove carbonates and Fe oxides and to ensure dispersion (Jackson, 1975). Excess electrolyte was removed by repeated centrifugations and when the suspension became stable, <0.2 µm fractions were separated by repeated centrifugations. One portion of the suspension was then flocculated with 1 N NaCl to reduce its volume, and another was exchanged four times with 1 N $CaCl_2$ (~100 mL/2 g of clay). Excess salts were removed by washings and subsequent dialysis, which was monitored by a conductivity meter. The purity of clay fractions was checked by X-ray diffraction (XRD) with a Scintag X1 diffractometer equipped with a solid-state Si detector. Scans from oriented sample preparations were made in air-dry states after equilibration in a 47% RH atmosphere in controlled-humidity chamber and after solvation with ethylene glycol vapor. Only trace amounts of impurities were detected in some samples and pure smectite composition (*i.e.* no detectable mixed layering) was confirmed by the rationality of 00l reflections (Table 2, available from the 'Deposited Material' section of journal pages on The Clay Minerals Society's website: www.clays.org/journal/JournalDeposits.html). Impurities at this low level do not affect the calculated smectite composition (*e.g.* no correlation of halite and K-feldspar presence with Na and K contents was observed in the corresponding smectite samples (compare data in Tables 1 and 2)).

Table 1. Structural formulae, $d_{06}$ from XRD, and values calculated from: total interlayer charge ($Q$), exchange cations (*EXCH*), fixed cations (*FIX*), volume of the unit cell ($V$), molecular weight per unit cell ($MW$), dry density ($d_s$), and total specific surface area (*TSSA*: see text for details).

| Data column | 1 | 2 | 3 | 4 | 5 | 6 | 7 | 8 | 9 | 10 | 11 | 12 |
| Sample | Si | $Al^{IV}$ | $Al^{VI}$ | $Fe^{3+}$ | Mg | Li | Sum VI | Layer charge | Ca | Na | K | $Q$ |
|---|---|---|---|---|---|---|---|---|---|---|---|---|
| Wyoming[1] | 3.88 | 0.12 | 1.54 | 0.21 | 0.25 | 0.00 | 2.00 | 0.37 | 0.18 | 0.01 | 0.01 | 0.37 |
| Mont. #20[2] | 3.80 | 0.20 | 1.39 | 0.34 | 0.30 | 0.00 | 2.03 | 0.42 | 0.20 | 0.02 | 0.00 | 0.41 |
| Chambers[3] | 4.00 | 0.00 | 1.38 | 0.09 | 0.54 | 0.00 | 2.02 | 0.49 | 0.24 | 0.01 | 0.00 | 0.49 |
| Texas[4] | 3.96 | 0.04 | 1.54 | 0.07 | 0.39 | 0.00 | 2.00 | 0.43 | 0.21 | 0.01 | 0.00 | 0.43 |
| Otay[5] | 3.97 | 0.03 | 1.33 | 0.07 | 0.66 | 0.00 | 2.06 | 0.51 | 0.25 | 0.01 | 0.00 | 0.50 |
| Cheto[6] | 4.00 | 0.00 | 1.39 | 0.09 | 0.54 | 0.00 | 2.02 | 0.48 | 0.23 | 0.02 | 0.01 | 0.48 |
| Kinney[7] | 3.92 | 0.08 | 1.50 | 0.08 | 0.43 | 0.00 | 2.01 | 0.48 | 0.23 | 0.01 | 0.00 | 0.48 |
| Ferr. Sm.[8] | 3.74 | 0.26 | 0.65 | 1.20 | 0.13 | 0.00 | 1.98 | 0.46 | 0.22 | 0.00 | 0.01 | 0.46 |
| Garfield[9] | 3.46 | 0.54 | 0.00 | 1.98 | 0.03 | 0.00 | 2.02 | 0.53 | 0.26 | 0.00 | 0.00 | 0.53 |
| Uley[10] | 3.80 | 0.20 | 0.27 | 1.62 | 0.05 | 0.00 | 1.93 | 0.45 | 0.21 | 0.01 | 0.01 | 0.45 |
| Hectorite[11] | 3.96 | 0.04 | 0.04 | 0.03 | 2.57 | 0.32 | 2.97 | 0.34 | 0.16 | 0.01 | 0.01 | 0.34 |
| Saponite[12] | 3.58 | 0.42 | 0.01 | 0.06 | 2.91 | 0.00 | 2.98 | 0.40 | 0.20 | 0.00 | 0.00 | 0.40 |
| Mean | | | | | | | | | | | | 0.45 |

| Data column (*cont.*) | 13 | 14 | 15 | 16 | 17 | 18 | 19 | 20 | 21 | 22 |
| Units | *EXCH* | *FIX* | $d_{06}$ nm | $V$ nm$^3$ | $MW$ g/mol | $d_s$ g/cm$^3$ | $TSSA_{Nr}$ m$^2$/g | $TSSA_N$ m$^2$/g | $TSSA_{EXCH}$ m$^2$/g | % diff |
|---|---|---|---|---|---|---|---|---|---|---|
| Wyoming[1] | 0.36 | 0.02 | 0.1500 | 0.4488 | 746.2 | 2.761 | 761.7 | 754.5 | 727.3 | −4.5 |
| Mont. #20[2] | 0.39 | 0.02 | 0.1500 | 0.4489 | 756.5 | 2.799 | 751.6 | 744.4 | 711.0 | −5.4 |
| Chambers[3] | 0.48 | 0.01 | 0.1500 | 0.4486 | 744.0 | 2.754 | 763.8 | 756.5 | 742.5 | −2.8 |
| Texas[4] | 0.42 | 0.01 | 0.1497 | 0.4472 | 739.8 | 2.747 | 765.6 | 758.4 | 745.1 | −2.7 |
| Otay[5] | 0.49 | 0.01 | 0.1501 | 0.4493 | 744.5 | 2.752 | 764.4 | 757.1 | 749.0 | −2.0 |
| Cheto[6] | 0.46 | 0.02 | 0.1499 | 0.4484 | 743.5 | 2.754 | 763.9 | 756.6 | 725.5 | −5.0 |
| Kinney[7] | 0.47 | 0.02 | 0.1496 | 0.4463 | 742.9 | 2.764 | 761.0 | 753.7 | 732.4 | −3.8 |
| Ferr. Sm.[8] | 0.45 | 0.01 | 0.1511 | 0.4556 | 805.6 | 2.936 | 716.3 | 709.5 | 698.7 | −2.5 |
| Garfield[9] | 0.52 | 0.01 | 0.1523 | 0.4630 | 855.8 | 3.070 | 685.2 | 678.7 | 673.7 | −1.7 |
| Uley[10] | 0.43 | 0.02 | 0.1516 | 0.4584 | 828.0 | 3.000 | 701.2 | 694.5 | 668.1 | −4.7 |
| Hectorite[11] | 0.32 | 0.02 | 0.1514 | 0.4576 | 762.5 | 2.767 | 760.2 | 753.0 | 707.2 | −7.0 |
| Saponite[12] | 0.40 | 0.01 | 0.1532 | 0.4686 | 776.4 | 2.752 | 764.4 | 757.2 | 752.7 | −1.5 |
| Mean | 0.43 | 0.02 | | 0.4534 | 770.5 | 2.821 | 746.6 | 739.5 | 719.4 | −3.6 |

[1] CMS montmorillonite SWy-1, [2] Ward's montmorillonite API#20, [3] Ward's montmorillonite Chambers API#23, [4] CMS montmorillonite Texas STx-1, [5] Ward's montmorillonite Otay API#24, [6] CMS montmorillonite Cheto SAz-1, [7] montmorillonite Kinney (Khoury and Eberl, 1981), [8] CMS ferruginous smectite SWa-1, [9] Ward's nontronite Garfield API#33, [10] CMS nontronite Uley NAu-2, [11] CMS hectorite SHCa-1, [12] CMS saponite Ballarat SapCa-1.
Sum VI: sum of octahedral cations

The $d_{06}$ values for all samples were accurately measured using calibrated XRD scans from random powders spiked with 10% of silicon powder (NIST SRM 640b) as internal standard (Table 1). Major-element chemical analyses of the clays in $Ca^{2+}$ and $[Co(NH_3)_6]^{3+}$ forms (referred to here as Ca-clays and Co-clays for simplicity) were obtained by inductively coupled plasma-atomic emission spectrometry (ICP-AES) from SGS Laboratories, Toronto, Canada. The analyses of Ca-clays were used for calculating structural formulae, and those of Co-clays for checking the completeness of $Ca^{2+}$ for $[Co(NH_3)_6]^{3+}$ exchange.

Comparing elemental analyses of the same samples from ICP-AES and X-ray fluorescence (XRF) techniques from the same laboratory (authors' unpublished data) revealed that ICP-AES is less precise than XRF with respect to $SiO_2$ and $Al_2O_3$. For this reason, in two cases for which obvious differences were noticed, the $SiO_2$ and $Al_2O_3$ from ICP-AES analyses available for <2 μm fractions of the same samples in $Na^+$ form (authors' unpublished data) was used (Wyoming and Garfield), which made the formulae similar to those published by Eberl *et al*. (1986) for the Wyoming sample and Gates *et al*. (2002) for Garfield. Conventional assignmnet of $Fe^{3+}$ to the octahedral sheet was applied because of the lack of data on partitioning, *e.g.* those of Gates *et al*. (2002) who assigned 0.05 and 0.14 to the octhedral sheet of Garfield and Uley, respectively. In the Texas smectite sample, 5.8% of amorphous silica that was detectable by FTIR was subtracted from the analysis to balance the formula. The theoretical occupancy of the octahedral sheet of two cations per $O_{10}(OH)_2$ was used as the criterion.

*Measurement of CEC, TSSA, and H<sub>2</sub>O retention*

The *CEC* was measured by the Co-hexamine technique on the Ca-exchanged smectite, following Bardon *et al.* (1983). In order to increase the accuracy of this determination, Co-exchanged clays were analyzed chemically for non-exchanged $Ca^{2+}$ and an appropriate correction was implemented (see the Results section).

The *TSSA* was measured using the standard free surface ethylene glycol monoethyl ether (EGME) adsorption technique of Tiller and Smith (1990) performed on the Ca-exchanged smectite. In both cases, two measurements were made for each sample and the results were averaged.

The $H_2O$ retention of smectite was investigated to develop an alternative *TSSA* measurement technique and to evaluate the content of $H_2O$ held by smectite at elevated temperatures. Thermal gravimetric analysis (TGA) combined with mass spectrometry (MS) evaluation of the evolved $H_2O$ was used. The TGA-MS experiments were conducted on smectite in Na and Ca forms, which are the dominant exchange cations found in natural smectite and are known to have different hydration properties (*e.g.* Hendricks *et al.*, 1940; Sato *et al.*, 1992; Ferrage *et al.*, 2005a, 2005b). Also, the smectite samples with $[Co(NH_3)_6]^{3+}$ exchange cations, produced in the course of *CEC* determination, were investigated.

The samples were equilibrated at 47% RH and ~25ºC over a saturated solution of lithium nitrate for 3 days in a sealed chamber to represent a typical air-dried state and two-layer $H_2O$ complex in the case of Ca smectite (MacEwan and Wilson, 1980; Newman, 1983; Watanabe and Sato, 1988; Sato *et al.*, 1992; Cases *et al.*, 1997;

Ferrage *et al.*, 2005a). Like EGME, $H_2O$ at low and medium RH covers only mineral surfaces and does not adsorb on the organic matter (Bigorre *et al.*, 2000).

The samples were placed in a platinum weighing pan and then placed immediately into the furnace of a TA Instruments© 2050 Thermogravimetric Analyzer equipped with a ThermoOnix© quadrupole mass spectrometer connected by a quartz capillary with a heated jacket at 180−200ºC to measure selected evolved-gas mass fragments. Helium was used under positive pressure as a carrier gas with a flow rate of 10 cm³/min. The relative intensity of the mass 18 signal reaching the spectrometer over the heating program of the TGA was used to qualitatively evaluate evolved $H_2O$ from the dehydration and dehydroxylation reactions compared to weight loss. The weight loss was measured at selected heating conditions and rates.

It is well known that not all clay mineral-bound $H_2O$ is lost during several hours of heating at 110ºC, which is the standard procedure used to dehydrate samples for *CEC* and *TSSA* analyses. Thus, in order to study the total bound water, a higher temperature has to be selected, but lower than the onset of dehydroxylation. The lowest dehydroxylation temperature for smectites was found to be approximately 250ºC, as occurs in the case of nontronite (Figure 1a; Examples of TGA curves for montmorillonite and saponite in Figures 1b and 1c are available from the 'Deposited Material' section of the journal pages on The Clay Minerals Society's website: www.clays.org/journal/JournalDeposits.html). The mass lost above this temperature, measured from the TGA curve, agrees with the theoretical content of 4.2% OH
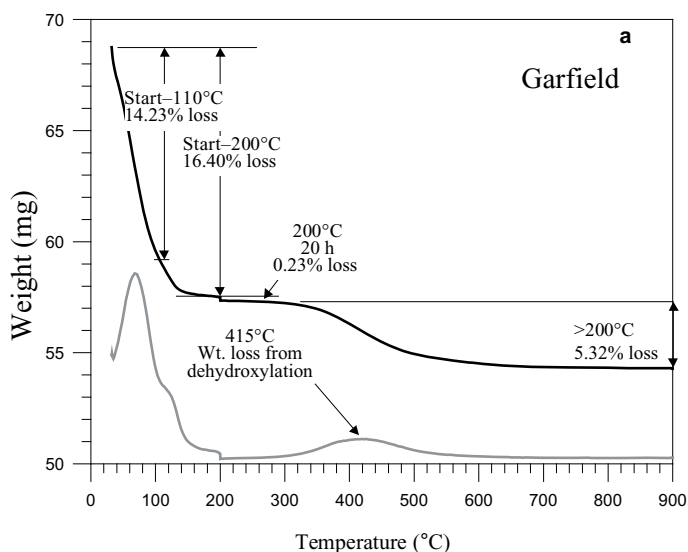


Figure 1. TGA-MS curves for representative Ca-smectites: (a) Garfield nontronite, (b) Wyoming montmorillonite, (c) Otay montmorillonite, (d) Ballarat saponite. Black curve = weight loss, gray curve = relative intensity of mass 18 spectrum. Weight changes from start to 110ºC, start to 200ºC, 200ºC for 20 h, and from 200ºC at 20 h to 900ºC at 1 h are shown (parts b, c, and d are available from the 'Deposited Material' section of journal pages on The Clay Minerals Society's website: www.clays.org/journal/JournalDeposits.html).

calculated from the nontronite formula; therefore nontronite dehydroxylation must start at 250ºC if no molecular water is present at this temperature, or below 250ºC if some molecular water is still present. Based on this and FTIR evidence of the onset of dehydroxylation (authors' unpublished data), 200ºC was selected as a safe temperature to use for evaluating the molecular $H_2O$ content, without fear of a contribution by dehydroxylation. To try to extract the $H_2O$ completely, prolonged heating (20 h at 200ºC) was applied. Therefore, for each sample, the heating program consisted of: (1) heating to 200ºC at 10ºC/min; (2) holding constant at 200ºC for 20 h; (3) increasing the temperature at 10ºC/min up to 900ºC; and (4) holding at this temperature for 1 h in order to ensure complete dehydroxylation.

## RESULTS

### $Q_s$ and TSSA from structural formulae

In the establishment of the structural formulae for the 12 analyzed smectite samples (Table 1), all Mg was assigned to the octahedral sheet. In the case of one sample only (saponite), the Ca exchange removed all the interlayer cations; in the remaining samples, small amounts of Na and K were detectable. The total interlayer charge of the clay mineral ($Q$) was assumed to be the sum of 2Ca + Na + K. Under the conditions of the exchange experiment, the Ca content represented the amount of exchangeable cations per $O_{10}(OH)_2$ (*EXCH*), and the Na + K, the amount of fixed cations (*FIX*). Under the simplifying assumption that the charge density of the fixed and expandable layers is the same, $Q$ can be regarded as $Q_s$, *i.e.* the smectitic interlayer charge. This is justified because of the small amount of fixed cations (*FIX*). Thus, the range of $Q_s$ obtained from the structural formulae was $0.34-0.53/O_{10}(OH)_2$ and the range of *EXCH* is $0.32-0.52$, corresponding to the underestimation of $Q_s$ by ~4%.

The molecular weights (*MW*, in g/mol) obtained from the formulae and the unit-cell dimensions were used to calculate the dry densities of the smectite samples:

$$d_s = \frac{MW}{A\nu \times V} \qquad (2)$$

where $V$ is the volume of the unit cell in $nm^3$, equal to $a \times b \times c \cdot \sin\beta$ for monoclinic structures and $A\nu$ is the coefficient of Avogadro's number (602.2). $a = b/3^{0.5}$, $b = 6 \times d_{06}$, and $c \cdot \sin\beta = d_{001} = t_s$ used in equation 1 = 0.96 nm for a fully dehydrated smectite. For dioctahedral clay minerals, $b$ (in nm) can also be calculated from $Fe/O_{10}(OH)_2$, using the regression of data from Table 1:

$$b = 0.0074 \times Fe + 0.898 \qquad R^2 = 0.97 \qquad (3)$$

Having $d_s$ from equation 2, the $TSSA_{Nr}$ values of all smectite samples were calculated (Table 1) using equation 1. A value of 100 nm was used as representa-

tive for the smectite particle radius ($r$), based on TEM measurements of Güven (1988). Varying this value within limits acceptable for smectite ($20-500$ nm) would not change $TSSA_{Nr}$ by more than 4%, and ignoring $r$ entirely results in *TSSA* (referred to here as $TSSA_N$) being lower by ~1% (Table 1). The latter was calculated using the relation

$$TSSA_N = \frac{2000 \times A\nu \times a \times b}{MW} \qquad (4)$$

which is a combination of equations 1 and 2.

The $TSSA_{Nr}$ of smectites was found to vary within a narrow range of $685-766$ $m^2/g$ (mean = 747). For dioctahedral smectites, *TSSA* is controlled by the Fe content (equation 5a), because of its effect on molecular weight (equation 5b) and $b$ (equation 3) and thus on $d_s$ (equation 2).

$$TSSA_{Nr} = -41.44 \times Fe + 767.27 \quad R^2 = 0.997 \qquad (5a)$$
$$MW = 58.00 \times Fe + 737.38 \quad R^2 = 0.997 \qquad (5b)$$

Our sample set represents the full range of Fe content in smectite, thus the calculated *MW*, $b$, $d_s$, and $TSSA_{Nr}$ represent the complete ranges of these parameters in natural smectites. The trioctahedral smectites have intermediate values.

The geometric calculation of $TSSA_{Nr}$ (equation 1) assumes that all interlayer cations are exchangeable, *i.e.* all interlayers are swelling. If Na + K are treated as fixed cations, the *TSSA* corresponding to the performed cationic exchange ($TSSA_{EXCH}$) is a few % less (Table 1, column 22). The $TSSA_{EXCH}$ values were calculated as $TSSA \times Ca/(Ca + K + Na)$, under the simplifying assumption that the *FIX* and *EXCH* correspond to the same layer charge.

### Smectite $H_2O$ retention

Table 3 contains selected $H_2O$-loss data obtained from the TGA-MS analysis and Figure 1 presents examples of TGA curves for low- and high-charge montmorillonite, nontronite, and saponite. These data demonstrate that $H_2O$ loss from all smectites follows the same trend and varies only in the details.

*$H_2O$ loss between 25ºC and 200ºC.* During heating up to 200ºC, smectite loses most of the adsorbed $H_2O$ molecules. For the Ca-smectite samples the loss varies from 14 to 18% of the original mass of the hydrated sample. The Na-smectite had the largest loss variability, $7-14\%$, with Co-smectite varying from 7.5 to 11.5%. Between 83 and 94% of this water was lost during heating up to 110ºC. Prolonged heating at a specified temperature produced only small additional $H_2O$ loss for Ca and Na-smectite. For example the mass of water evolved during 20 h of heating at 200ºC was <2% of the $H_2O$ lost up to this temperature, or $0.14-0.42\%$ of the original sample mass (Table 3). This $H_2O$ loss was independent of the charge density of the smectite. The

Table 3. Initial weight and weight losses (reported as % of the initial weight) recorded from TGA-MS for Ca, Na, and Co-clays. *WBW* compared to theoretical monolayer coverage $H_2O_{mono}$ calculated using equation 6. Co as used here means $Co[(NH_3)_6]^{3+}$, see text.

| Data column | 1 | 2 | 3 | 4 | 5 | 6 | 7 | 8 | 9 | 10 |
|---|---|---|---|---|---|---|---|---|---|---|
| Sample | Initial sample weight Ca | $H_2O_{mono}$ from eq. 6 | $WBW_{Ca}$: Intial $-200°C$ | $WBW_{Ca}$ as % $H_2O_{mono}$ | Initial sample weight Na | $WBW_{Na}$: Initial $-200°C$ | $WBW_{Na}$ as % $H_2O_{mono}$ | Initial sample weight Co | $WBW_{Co}$: Initial $-200°C$ | $WBW_{Co}$ as % $H_2O_{mono}$ |
| Units | mg | wt.% | wt.% | % | mg | wt.% | % | mg | wt.% | % |
| Wyoming | 33.592 | 17.87 | 14.25 | 79.75 | 51.360 | 8.07 | 45.15 | 28.600 | 7.52 | 42.07 |
| Mont. #20 | 66.905 | 17.67 | 15.73 | 89.01 | 57.920 | 12.34 | 69.82 | 50.582 | 10.38 | 58.73 |
| Chambers | 91.570 | 17.91 | 15.73 | 87.84 | 88.537 | 12.34 | 68.91 | 50.779 | 10.38 | 57.96 |
| Texas | 61.408 | 17.94 | 15.05 | 83.87 | 81.583 | 10.81 | 60.24 | 52.960 | 8.56 | 47.72 |
| Otay | 81.490 | 17.92 | 18.23 | 101.73 | 94.139 | 14.34 | 80.02 | 73.078 | 11.01 | 61.44 |
| Cheto | 100.596 | 17.91 | 17.46 | 97.49 | 81.851 | 13.27 | 74.09 | 85.753 | 10.87 | 60.69 |
| Kinney | 102.181 | 17.85 | 17.43 | 97.62 | 55.600 | 12.16 | 68.11 | 67.100 | 10.89 | 60.99 |
| Ferr. Sm. | 129.980 | 16.98 | 15.39 | 90.61 | 85.182 | 11.32 | 66.65 | 46.463 | 11.56 | 68.06 |
| Garfield | 68.757 | 16.37 | 16.40 | 100.20 | 49.771 | 10.45 | 63.84 | 49.486 | 10.53 | 64.33 |
| Uley | 47.033 | 16.69 | 14.86 | 89.06 | 49.032 | 6.92 | 41.48 | 51.121 | 9.76 | 58.47 |
| Hectorite | 66.062 | 17.84 | 15.45 | 86.61 | 69.625 | 11.61 | 65.08 | 34.359 | 8.96 | 50.22 |
| Saponite | 64.169 | 17.92 | 15.49 | 86.44 | 58.801 | 11.97 | 66.79 | 54.757 | 8.51 | 47.49 |
| Mean | | 17.57 | 15.96 | 90.85 | | 11.30 | 64.18 | | 9.91 | 56.52 |

| Data column (*cont.*) | 11 | 12 | 13 | 14 | 15 | 16 |
|---|---|---|---|---|---|---|
| Sample | Intial$-110°C$ Ca wt.% | Initial$-110°C$ Na wt.% | Initial$-110°C$ Co wt.% | 200°C$-200°C$ after 20 h Ca wt.% | 200°C$-200°C$ after 20 h Na wt.% | 200°C$-200°C$ after 20 h Co wt.% |
| Wyoming | 12.81 | 7.52 | 6.36 | 0.24 | 0.42 | 0.52 |
| Mont. #20 | 13.79 | 11.41 | 8.68 | 0.24 | 0.26 | 0.76 |
| Chambers | 14.32 | 12.45 | 8.49 | 0.14 | 0.22 | 0.79 |
| Texas | 13.07 | 10.79 | 7.18 | 0.17 | 0.14 | 0.53 |
| Otay | 15.00 | 13.51 | 8.59 | 0.20 | 0.15 | 0.99 |
| Cheto | 14.00 | 12.39 | 8.69 | 0.21 | 0.24 | 0.77 |
| Kinney | 13.80 | 11.66 | 8.90 | 0.23 | 0.17 | 0.64 |
| Ferr. Sm. | 12.53 | 10.78 | 9.69 | 0.28 | 0.16 | 0.67 |
| Garfield | 14.23 | 9.87 | 8.24 | 0.23 | 0.20 | 0.63 |
| Uley | 13.29 | 6.39 | 8.04 | 0.17 | 0.21 | 0.44 |
| Hectorite | 13.76 | 10.31 | 8.00 | 0.22 | 0.25 | 0.27 |
| Saponite | 13.45 | 11.16 | 7.28 | 0.18 | 0.26 | 0.35 |
| Mean | 13.67 | 10.69 | 8.18 | 0.21 | 0.22 | 0.61 |

rate of $H_2O$ loss during isothermal heating decreased logarithmically with time (Figure 2). In order to evolve more $H_2O$ in a reasonably short time the temperature must, therefore, be increased. The Co-smectites behaved differently, with a mass loss during isothermal heating up to 200°C of up to 6% due to evolved $H_2O$ (Table 3).

The amount of $H_2O$ lost by smectites equilibrated at 47% RH up to 200°C, referred to here as weakly bound water (*WBW* in Table 3), can be used for the *TSSA* evaluation if it is close to the monolayer coverage of smectite surfaces, which corresponds to one water layer on the outside crystal surfaces and two water layers in the interlayers. According to Newman (1983), Watanabe and Sato (1988), and Sato *et al.* (1992), this is the case for Ca-smectite at intermediate RH levels.

In order to evaluate the experimental data from this standpoint, the theoretical monolayer coverage was calculated. The calculation assumed that a circular particle of radius $r$ (nm) and thickness $N \times t_s$ (nm) is covered on all sides by a monomolecular layer of $H_2O$ with a thickness $t_w$ (nm) and density $d_w$ (g/cm$^3$):

$$\frac{H_2O_{mass}}{dryclay_{mass}} = \frac{(2\pi r^2 \times t_w + 2\pi r N t_s \times t_w) \times d_w}{\pi r^2 N t_s \times d_s}$$

The mass of $H_2O$ ($H_2O_{mass}$) + the mass of dry clay ($dryclay_{mass}$) = the mass of air-dried clay at 47% RH (*air-dried clay$_{mass}$*). Combining these two equations and setting *air-dried clay$_{mass}$* as 100%, we obtain the equation for theoretical monolayer water coverage
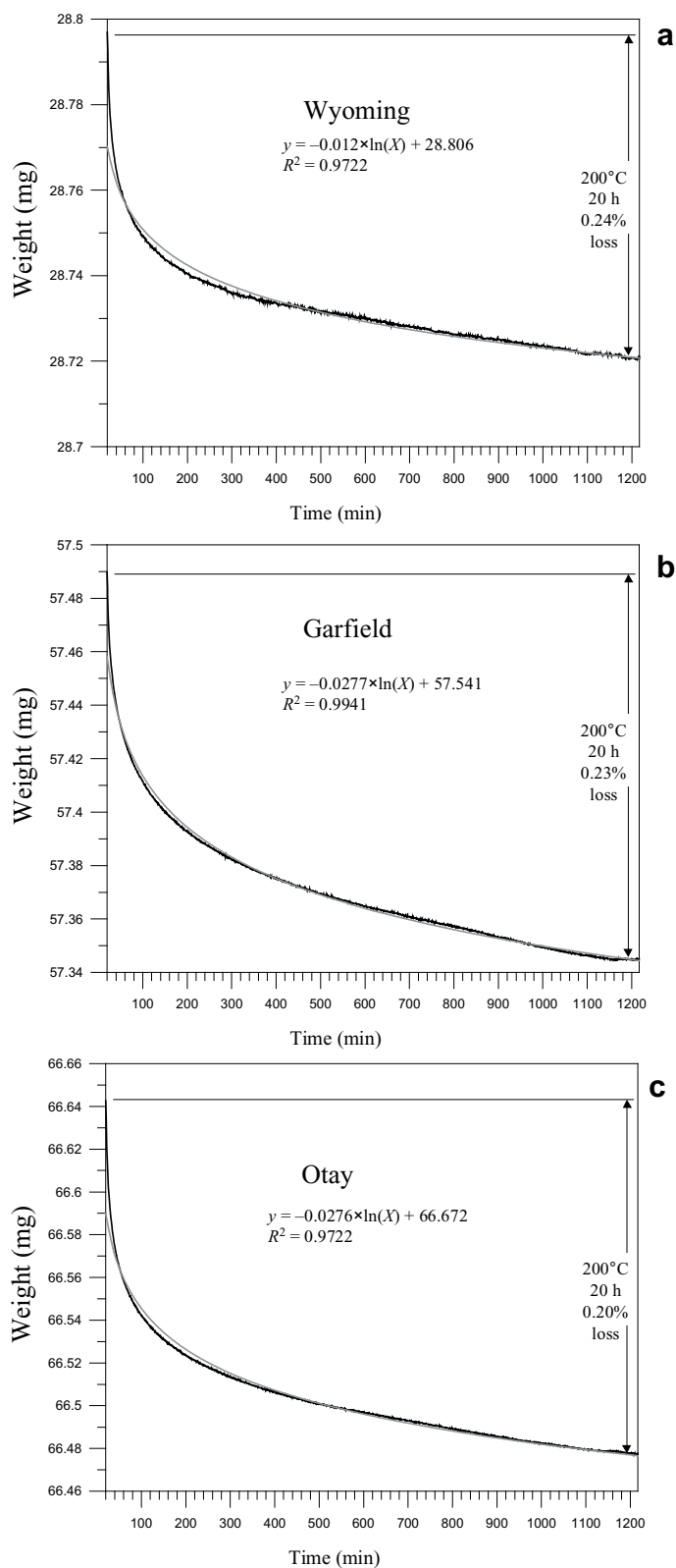
Figure 2. Weight loss of representative Ca smectites due to dehydration during 200ºC isothermal heating for 20 h: black curve = experimental data, gray curve = fitted logarithmic curve (a: Wyoming montmorillonite; b: Garfield nontronite; c: Otay montmorillonite).

($H_2O_{mono}$), expressed, like the experimental measurement, as the % of the original mass:

$$H_2O_{mono} = \frac{100}{\left( \dfrac{d_s}{2t_s d_w \times (1/N t_s + 1/r)} + 1 \right)} \qquad (6)$$

where $t_s$ = 0.96 nm (monolayers), $r$ is on the order of 100 nm, and $t_w$ = 0.286 nm. The precise value of $t_w$ was calculated from $t_s$ and $d_{001}$ of the Ca-smectite at 47% RH, obtained from equation 11 of Ferrage *et al.* (2005a). The effect of $r$ on the calculation is small, so using an approximate number is justified. In this calculation, the density of $H_2O$ in the monolayer is accepted as equal to the liquid water density (1 g/cm$^3$).

The results of the calculation in equation 6 are presented in Table 3 (column 2) along with the experimental data (*WBW*). The experimental data for Ca-smectites are close (80−100%) to the theoretical monolayer coverage, which confirms earlier findings of Newman (1983), Watanabe and Sato (1988), and Sato *et al.* (1992). The corresponding values for the Na- and Co-smectite samples are 41−80% and 42−68%, respectively.

The conclusions based on the theoretical monolayer coverage approach are consistent with the XRD evidence. The $d_{001}$ of all Ca-smectite samples under investigation were recorded at 47% RH (Table 2) and are between 14.2 and 15.6 Å, which is characteristic of the dominant two-layer $H_2O$ complex (*e.g.* Brindley and Brown, 1980). In some samples, an almost perfect two-layer complex was observed, as shown by the $d_{005} \times 5$ value that is close to the $d_{001}$ value (Table 2).

A smaller percentage of monolayer coverage for Na- and Co-smectite indicates a significant proportion of smectite layers with a single-layer $H_2O$ complex in the interlayer, which would have a $d_{001}$ of ~12.5 Å for an ideal single $H_2O$ layer structure (Brindley and Brown, 1980). Indeed, the $d_{001}$ values recorded at 47% RH varied from 12.4 to 14.2 Å for Na-smectite samples (Table 2). These XRD characteristics indicated a large variation of $H_2O$ content in Na-smectite when compared with Ca-smectite, which is consistent with the TGA measurements.

The data in Table 3 suggest that $H_2O$ held by Ca-smectite at 47% RH can be accounted for by essentially complete monomolecular coverage of the total surface area of clay. For each interlayer cation, the amount of $H_2O$ is positively correlated with charge density but this correlation is weak (Figure 3a: available from the 'Deposited Material' section of journal pages on The Clay Minerals Society's website: www.clays.org/journal/JournalDeposits.html). No correlation with the amount of tetrahedral charge was observed (Figure 3b: available from the 'Deposited Material' section of journal pages on The Clay Minerals Society's website: www.clays.org/journal/JournalDeposits.html). These findings encourage the use of $H_2O$ released from Ca-smectite up to 200ºC as a means by which to measure *TSSA*. Such an approach has

greater potential than using the $H_2O$ released at 110ºC because the latter accounts for only 86% of the monomolecular coverage (Table 3, columns 2 and 11).

*$H_2O$ loss above 200ºC.* The weight loss above 200ºC, when recalculated as the percentage of the total weight minus the weight lost after 20 h at 200ºC (Table 4, column 2), is greater than the theoretical OH content of smectite, calculated from their structural formulae (Table 4, column 1). This difference, or excess weight, is interpreted in this study as an approximate weight of the $H_2O$ tightly bound to the smectite structure (Table 4, column 3). It is only an approximate value, because the weight loss above 200ºC is expressed at the weight on a 200ºC basis, while the OH content is calculated on water-free basis. This approximate value can be further refined by recalculating the OH content to the weight on a 200ºC basis (Table 4, column 4), *i.e.* by taking into account the dilution effect of the tightly bound $H_2O$, based on its approximate weight. The final weight of the tightly bound $H_2O$ (*TBW*) calculated following this approach is presented in Table 4 (columns 5−8) as: (1) the percentage of the dry weight; (2) percentage of the air-dry weight; (3) as the weight fraction of the structural OH groups; and (4) as the number of moles per molecular weight of smectite.

In Ca- and Na-smectite, the *TBW* values are very similar and well correlated (Table 4, columns 8 and 9). The Ca-smectite contains slightly less *TBW* than the Na-smectite (0.56 compared to 0.62 mole/*MW*). The corresponding values for Co-smectite are more than two times higher (column 10). Thus the *TBW* content is clearly controlled by the nature of the exchangeable cation. The relationship to layer charge is not observed for Co-smectite and is weak and negative for Ca and Na smectite (Figure 4, available from the 'Deposited Material' section of journal pages on The Clay Minerals Society's website: www.clays.org/journal/JournalDeposits.html).

*Total $H_2O$ loss and $H_2O$ molecular area on smectite surface.* For practical reasons the sum of *TBW* (from Table 4), and the molecular $H_2O$ lost during prolonged heating at 200ºC (last columns in Table 3), can be expressed as a fraction, $f_{SBW}$, of the $H_2O$ lost up to 200ºC, which is referred to here as weakly bound $H_2O$, *WBW* (Table 3). This factor is variable, but significant, ranging from an average value of 0.08 for Ca-smectite to 0.14 for Na-smectite (Table 5).

When the $f_{SBW}$ value is known, the total $H_2O$ released from smectite equilibrated at 47% RH (*BW*) can be calculated from the $H_2O$ loss at 200ºC, which is easily measurable:

$$BW = WBW \times (1 + f_{SBW}) \qquad (7)$$

This calculation shows that both Co- and Na-smectite are characterized at 47% RH by a similar amount of total

Table 4. Molecular water released by smectite above 200ºC ($TBW$), calculated from theoretical OH content and TGA-MS weight loss above 200ºC. Complete calculation presented for Ca smectite (details in the text). $TBW$ expressed as wt.% of dry weight (20 h at 200ºC) and air weight, as fraction of OH content of the smectite, and as number of moles per molecular weight.

| Data column | 1 | 2 | 3 | 4 | 5 | 6 | 7 | 8 | 9 | 10 |
|---|---|---|---|---|---|---|---|---|---|---|
| Sample | Theor. %OH in Ca-Sm | $H_2O$ loss above 200ºC Ca-Sm | Approx. excess $H_2O$ Ca-Sm | %OH in dry Ca-Sm | $TBW_{Ca}$ as % dry weight | $TBW_{Ca}$ as % air-dried weight | $TBW_{Ca}$ as fraction OH | $TBW_{Ca}$ as mol/$MW$ | $TBW_{Na}$ as mol/$MW$ | $TBW_{Co}$ as mol/$MW$ |
| Units | wt.% | wt.% | wt.% | wt.% | wt.% | wt.% | | mol/$MW$ | mol/$MW$ | mol/$MW$ |
| Wyoming | 4.83 | 6.64 | 1.81 | 4.74 | 1.90 | 1.62 | 0.40 | 0.80 | 1.06 | 1.39 |
| Mont. #20 | 4.76 | 6.22 | 1.46 | 4.69 | 1.52 | 1.28 | 0.32 | 0.65 | 0.73 | 1.28 |
| Chambers | 4.84 | 5.90 | 1.06 | 4.79 | 1.11 | 0.94 | 0.23 | 0.46 | 0.41 | 1.32 |
| Texas | 4.87 | 5.58 | 0.71 | 4.84 | 0.74 | 0.63 | 0.15 | 0.31 | 0.23 | 1.07 |
| Otay | 4.84 | 5.77 | 0.93 | 4.79 | 0.97 | 0.79 | 0.20 | 0.41 | 0.30 | 1.12 |
| Cheto | 4.85 | 5.94 | 1.09 | 4.79 | 1.14 | 0.94 | 0.24 | 0.48 | 0.50 | 1.27 |
| Kinney | 4.85 | 5.50 | 0.65 | 4.82 | 0.68 | 0.56 | 0.14 | 0.28 | 0.27 | 1.20 |
| Ferr. Sm. | 4.47 | 5.46 | 0.99 | 4.43 | 1.03 | 0.87 | 0.23 | 0.47 | 0.29 | 1.02 |
| Garfield | 4.21 | 5.32 | 1.11 | 4.16 | 1.16 | 0.97 | 0.28 | 0.56 | 0.45 | 1.67 |
| Uley | 4.35 | 6.47 | 2.11 | 4.26 | 2.20 | 1.87 | 0.52 | 1.04 | 0.82 | 1.45 |
| Hectorite | 4.73 | 6.26 | 1.54 | 4.65 | 1.61 | 1.36 | 0.35 | 0.69 | 0.78 | 1.20 |
| Saponite | 4.64 | 5.91 | 1.27 | 4.58 | 1.33 | 1.12 | 0.29 | 0.58 | 1.65 | 1.39 |
| Mean | 4.69 | 5.91 | 1.23 | 4.63 | 1.28 | 1.08 | 0.28 | 0.56 | 0.62 | 1.28 |

surface-bound $H_2O$, ~74% of the monomolecular coverage, while Ca-smectite contains, on average, 98% of the monomolecular $H_2O$ coverage, with variation between 88 and 107%, which corresponds to $8-10$ mol of $H_2O$ per $MW$ of smectite (Table 5).

The result obtained for Ca-smectite was confirmed by an alternative calculation based on the molecular area of $H_2O$ ($a_{H_2O}$). The molecular area, or the surface area represented by an $H_2O$ molecule, was calculated in two ways: (1) from the equation for two-dimensional close packing (equation 2 in Chiou *et al.*, 1993); and (2) from the thickness, $t_w$, of the $H_2O$ layer on a smectite surface, used in equation 6, assuming the $H_2O$ density on the surface, $d_w$ equals liquid density:

$$a_{H_2O} = \frac{MW \times 10^{21}}{t_w \times d_w \times Av} \qquad (8)$$

Table 5. Fractions of strongly bound water ($f_{SBW}$) and all bound water ($BW$) calculated using equation 7 and expressed as percentage of theoretical monolayer coverage. For Ca-smectite also the raw BW number and $BW$ expressed as number of moles of $H_2O$ per $MW$ is listed. The last two columns present an alternative calculation of $WBW$ and $BW$ for Ca clays using equation 9 and the molecular area of water ($a_{H_2O}$) established from equation 8.

| Data column Sample | 1 $f_{SBW}$ Ca-Sm | 2 $f_{SBW}$ Na-Sm | 3 $f_{SBW}$ Co-Sm | 4 $BW_{Ca}$ | 5 $BW$ as mol/$MW$ | 6 $BW_{Ca}$ as % mono | 7 $BW_{Na}$ as % mono | 8 $BW_{Co}$ as % mono | 9 $WBW_{Ca}$ as % mono from $a_{H_2O}$ | 10 $BW_{Ca}$ as % mono. from $a_{H_2O}$ |
|---|---|---|---|---|---|---|---|---|---|---|
| Units | | | | wt.% | mol/$MW$ | % | % | % | % | % |
| Wyoming | 0.13 | 0.33 | 0.46 | 16.11 | 7.96 | 90 | 60 | 62 | 76 | 88 |
| Mont. #20 | 0.10 | 0.14 | 0.33 | 17.25 | 8.75 | 98 | 80 | 78 | 87 | 97 |
| Chambers | 0.07 | 0.09 | 0.34 | 16.80 | 8.34 | 94 | 75 | 78 | 86 | 93 |
| Texas | 0.05 | 0.06 | 0.33 | 15.85 | 7.73 | 88 | 64 | 64 | 81 | 86 |
| Otay | 0.05 | 0.05 | 0.30 | 19.23 | 9.84 | 107 | 84 | 80 | 102 | 109 |
| Cheto | 0.07 | 0.10 | 0.31 | 18.61 | 9.44 | 104 | 81 | 80 | 97 | 105 |
| Kinney | 0.05 | 0.06 | 0.29 | 18.23 | 9.19 | 102 | 72 | 79 | 97 | 103 |
| Ferr. Sm. | 0.07 | 0.06 | 0.23 | 16.54 | 8.86 | 97 | 71 | 84 | 89 | 97 |
| Garfield | 0.07 | 0.10 | 0.35 | 17.59 | 10.14 | 107 | 70 | 87 | 100 | 109 |
| Uley | 0.14 | 0.27 | 0.33 | 16.90 | 9.35 | 101 | 53 | 78 | 87 | 102 |
| Hectorite | 0.10 | 0.16 | 0.31 | 17.03 | 8.69 | 95 | 75 | 66 | 84 | 95 |
| Saponite | 0.08 | 0.29 | 0.38 | 16.78 | 8.69 | 94 | 86 | 65 | 84 | 92 |
| Mean | 0.08 | 0.14 | 0.33 | 17.24 | 8.91 | 98 | 73 | 75 | 89 | 98 |

Both calculations produced almost identical $a_{H_2O}$ (0.1050 and 0.1047 nm² respectively). The percentage of monolayer coverage (%$_{mono}$) was calculated with $a_{H_2O}$ = 0.105 nm following equation 1 of Newman (1983):

$$\%_{mono} = \frac{a_{H_2O} \times Av \times m_{H_2O}}{MW \times TSSA_{Nr} \times 10^{19}} \quad (9)$$

where ($m_{H_2O}$) (mg/g) is $H_2O$ retention in Ca-smectite equilibrated at 47% RH. The result of this calculation is close to that obtained using equation 6 (Table 5). If $m_{H_2O}$ used in equation 9 corresponds to *WBW* (mg of $H_2O$ evolved up to 200°C, divided by the weight of clay mineral at 200°C), the average amount of monomolecular coverage is 89%. The value increases to 91% if dry weight (the weight of clay at 200°C corrected for $H_2O$ left in the clay) is used as the reference in the $m_{H_2O}$ calculation. If *BW* is used to calculate $m_{H_2O}$, the average monolayer coverage increases to 98% (Table 5).

The $H_2O$ data obtained for Ca-smectite are used below for the refinement of *CEC* and *TSSA* measurements.

*Comparison of Q and EXCH from CEC and structural formula*

In smectite, the layer charge, *Q*, would strictly correspond to the *CEC* if all the cations satisfying the charge were exchangeable. If this is not the case, then *CEC* corresponds to *EXCH*. The *CEC*, which is defined as the amount of exchangeable cations per unit weight of the sample, is then equivalent to 2·*EXCH*/*MW* (2·*EXCH* because *EXCH* refers to $O_{10}(OH)_2$). A factor of 100,000 has to be used to convert from meq/100 g (units of *CEC*) to *eq*/g (units of *EXCH*/*MW*). Thus:

$$EXCH = \frac{CEC \times MW}{200,000} \quad (10)$$

An equivalent calculation of $Q_s$ can be made using *CEC* and $TSSA_{EXCH}$, because the smectitic layer charge is the ratio between the amount of exchangeable cations and the surface accessible to these cations, and both *CEC* and $TSSA_{EXCH}$ express these values per unit mass:

$$Q_S = \frac{CEC(\text{meq}/100 \text{ g})}{TSSA_{EXCH}} = \frac{CEC}{100,000 \times TSSA_{EXCH}}$$

In order to convert eq/m² (units of $Q_s$ in the above equation) into eq per half molecular weight of smectite (units of $Q_s$ as defined in this paper), we have to multiply by the surface area corresponding to the mass of half the molecular weight: $a \times b \times 6.022 \times 10^{23}$ nm² and then convert to meters:

$$Q_S = \frac{CEC \times b^2 \times 3.477}{TSSA_{EXCH}} \quad (11)$$

This calculation slightly underestimates $Q_s$ because the unit conversion is performed under the assumption that all charge comes only from basal surfaces of clay mineral fundamental particles. This underestimation corresponds to the difference between $TSSA_{Nr}$ and $TSSA_N$, which is ~1% for *r* = 100 nm (Table 1). The discrepancy decreases to 0.5% for *r* = 200 nm and increases to 1.3% for *r* = 70 nm. In order to correct for this effect, a mean multiplication factor of 1.01 has been used in the calculations presented in Table 6.

An experimental problem inherent to the application of equations 10 and 11 results from the fact that *MW* and $TSSA_{EXCH}$ correspond to the theoretical $H_2O$-free mass of smectite, while *CEC* has been measured by standard procedure on a 110°C basis. Thus, in order to make *CEC* compatible with *MW* and $TSSA_{EXCH}$, the measured *CEC* value should be corrected to a $H_2O$-free basis using the data from Tables 3 and 4. Table 6 presents the *CEC* measurements and the results of $Q_s$ and *EXCH* calculations both with and without the correction for strongly bound $H_2O$.

The calculations without correction show that both equations produce values close to those evaluated from structural formulae, but that are systematically underestimated. $Q_s$ is greater than *EXCH* and the difference between the two is similar to that between the formula-derived values (Tables 1 and 6).

Correcting *CEC* for the $H_2O$ left in the smectite at 110°C ($CEC_{corr}$) reduces the underestimation of *EXCH* and $Q_s$ (Table 1 and Table 6). The regressions obtained for these data (Figure 5) indicate that the underestimations almost disappear for high $Q_s$ and *EXCH* values, but remain for smaller values. The mean difference between the calculations of *EXCH* and $Q_s$, based on the structural formula and $CEC_{corr}$ is small (3.9%). The discrepancy can be reduced to 2.5% if $CEC_{corr}$ is further corrected to account for the incomplete exchange of Ca during the Co-hexamine standard procedure ($CEC_{corr2}$ in Table 6). Inductively coupled plasma analysis of the exchange product revealed that ~0.5−4.5% of the original Ca remained on the clay. This Ca was recalculated into an equivalent amount of $Co(NH_3)_6$ and then added to the *CEC* to produce $CEC_{corr2}$ (Table 6).

*TSSA calculations from $H_2O$ and EGME sorption*

*TSSA from $H_2O$ content at 47% RH.* It was shown above (Table 3) that the mass of $H_2O$ released during heating of Ca-smectite samples to 200°C is close to the monomolecular coverage. This portion of the absorbed $H_2O$ was then used to measure the *TSSA*. The relevant calculations are presented in Table 7. The mass of $H_2O$ released during heating to 200°C was calculated in two ways using the data from Table 3: (1) with respect to the mass of clay at 200°C (air-dried mass − mass of *WBW*); and (2) with respect to the mass of dry clay (air-dried mass − mass of *BW*). From these values and $TSSA_{Nr}$ (Table 1), the corresponding masses of $H_2O$ per 1 m² were obtained.

Table 6. Calculation of exchangeable cations ($EXCH$) and interlayer charge ($Q_s$) using equations 10 and 11 and employing $CEC$ measured and $CEC$ corrected for water held in smectite at 110°C. The second correction ($CEC_{corr2}$) accounts for % Ca left on the smectite after Co-hexamine treatment. The column '% diff' represents the relative difference between $EXCH$ and $Q_s$ calculated from $CEC$ and the relevant values calculated from the structural formula.

| Data column | 1 | 2 | 3 | 4 | 5 | 6 | 7 | 8 | 9 | 10 | 11 | 12 |
|---|---|---|---|---|---|---|---|---|---|---|---|---|
| Sample | $CEC_{meas}$ | $EXCH$ from $CEC_{meas}$ | $Q_s$ from $CEC_{meas}$ | $CEC_{corr}$ | $EXCH$ from $CEC_{corr}$ | $Q_s$ from $CEC_{corr}$ | % diff | %Ca not exch. by Co | $CEC_{corr2}$ | $EXCH$ from $CEC_{corr2}$ | $Q_s$ from $CEC_{corr2}$ | % diff |
| Units | meq/100 g | | | meq/100 g | | | % | % | meq/100 g | | | % |
| Wyoming | 85.64 | 0.32 | 0.33 | 89.01 | 0.33 | 0.35 | −6.8 | 1.13 | 90.03 | 0.34 | 0.35 | −5.75 |
| Mont. #20 | 94.64 | 0.36 | 0.38 | 98.60 | 0.37 | 0.39 | −4.8 | 1.13 | 99.72 | 0.38 | 0.40 | −3.70 |
| Chambers | 122.36 | 0.46 | 0.47 | 126.02 | 0.47 | 0.48 | −2.4 | 0.92 | 127.19 | 0.47 | 0.49 | −1.54 |
| Texas | 102.34 | 0.38 | 0.39 | 105.71 | 0.39 | 0.40 | −6.0 | 2.24 | 108.13 | 0.40 | 0.41 | −3.86 |
| Otay | 122.84 | 0.46 | 0.47 | 129.27 | 0.48 | 0.49 | −2.2 | 1.82 | 131.67 | 0.49 | 0.50 | −0.37 |
| Cheto | 118.82 | 0.44 | 0.47 | 125.54 | 0.47 | 0.49 | 1.8 | 1.45 | 127.39 | 0.47 | 0.50 | 3.33 |
| Kinney | 118.11 | 0.44 | 0.46 | 124.50 | 0.46 | 0.48 | −0.6 | 1.43 | 126.31 | 0.47 | 0.49 | 0.81 |
| Ferr. Sm. | 99.33 | 0.40 | 0.41 | 104.11 | 0.42 | 0.43 | −6.1 | 3.59 | 107.98 | 0.43 | 0.45 | −2.59 |
| Garfield | 115.48 | 0.49 | 0.50 | 120.19 | 0.51 | 0.52 | −0.4 | 0.47 | 120.75 | 0.52 | 0.53 | 0.09 |
| Uley | 90.96 | 0.38 | 0.40 | 94.91 | 0.39 | 0.41 | −8.4 | 4.51 | 99.39 | 0.41 | 0.43 | −4.04 |
| Hectorite | 80.56 | 0.31 | 0.33 | 83.73 | 0.32 | 0.34 | 0.7 | 0.69 | 84.31 | 0.32 | 0.35 | 1.44 |
| Saponite | 91.98 | 0.36 | 0.36 | 95.67 | 0.37 | 0.38 | −6.7 | 4.46 | 100.13 | 0.39 | 0.39 | −2.34 |
| Mean | 103.59 | 0.40 | 0.41 | 108.10 | 0.42 | 0.43 | 3.9 | 1.99 | 110.25 | 0.42 | 0.44 | 2.49 |

Table 7. Alternative *TSSA* calculations based on *WBW* (Table 3) and resulting relative errors with respect to *TSSA*$_{Nr}$ values obtained from structural formulae in Table 1 (see text for details).

| Data column | 1 | 2 | 3 | 4 | 5 | 6 | 7 | 8 | 9 | 10 | 11 | 12 | 13 |
|---|---|---|---|---|---|---|---|---|---|---|---|---|---|
| Sample | *WBW* as mg H$_2$O per g smectite (200°C) | *WBW* as mg H$_2$O per g of dry smectite | mg H$_2$O/m$^2$ (200°C) | mg H$_2$O/m$^2$ (dry) | *TSSA* from mg H$_2$O/m$^2$ (200°C) | % error | *TSSA* from mg H$_2$O/m$^2$ (dry) | % error | *TSSA* from mg H$_2$O/m$^2$ (dry) refined by CEC/*TSSA*$_{Tr}$ | % error | WBW/ *TSSA* | *TSSA* from WBW/*TSSA* | % error |
| Units | mg/g | mg/g | mg/m$^2$ | mg/m$^2$ | m$^2$/g | % | m$^2$/g | % | m$^2$/g | % | | m$^2$/g | % |
| Wyoming | 166 | 170 | 0.218 | 0.223 | 652 | −14 | 657 | −14 | 724 | −5 | 0.019 | 666 | −13 |
| Mont. #20 | 187 | 190 | 0.248 | 0.253 | 733 | −3 | 735 | −2 | 765 | 2 | 0.021 | 735 | −2 |
| Chambers | 187 | 189 | 0.244 | 0.248 | 733 | −4 | 731 | −4 | 686 | −10 | 0.021 | 735 | −4 |
| Texas | 177 | 179 | 0.231 | 0.234 | 695 | −9 | 691 | −10 | 711 | −7 | 0.020 | 704 | −8 |
| Otay | 223 | 226 | 0.292 | 0.295 | 875 | 14 | 872 | 14 | 812 | 6 | 0.024 | 852 | 11 |
| Cheto | 212 | 215 | 0.277 | 0.281 | 830 | 9 | 829 | 9 | 771 | 1 | 0.023 | 816 | 7 |
| Kinney | 211 | 213 | 0.277 | 0.280 | 828 | 9 | 824 | 8 | 773 | 2 | 0.023 | 815 | 7 |
| Ferr. Sm. | 182 | 184 | 0.254 | 0.257 | 714 | 0 | 713 | 0 | 716 | 0 | 0.021 | 719 | 0 |
| Garfield | 196 | 199 | 0.286 | 0.290 | 770 | 12 | 769 | 12 | 703 | 3 | 0.024 | 767 | 12 |
| Uley | 175 | 179 | 0.249 | 0.255 | 685 | −2 | 691 | −1 | 711 | 1 | 0.021 | 695 | −1 |
| Hectorite | 183 | 186 | 0.240 | 0.245 | 717 | −6 | 720 | −5 | 806 | 6 | 0.020 | 722 | −5 |
| Saponite | 183 | 186 | 0.240 | 0.244 | 719 | −6 | 719 | −6 | 780 | 2 | 0.020 | 724 | −5 |
| Mean | 190 | 193 | 0.255 | 0.259 | 746 | 7 | 746 | 7 | 747 | 4 | 0.021 | 746 | 6 |

The mean values calculated in this way are close to the value of 0.286 mg/m$^2$, representing monomolecular coverage of the surface (0.286 nm layer of density equal 1g/cm$^3$), calculated from $t_w$ assumed in equation 6.

The mean H$_2$O coverage values were used to calculate $TSSA$ from the measured masses of H$_2$O released during heating. The calculations give close results, which implies that heating to 200ºC is sufficient for the estimation of $TSSA$ by this technique. The average error of the measurement calculated with respect to $TSSA_{Nr}$ from Table 1 is ~7%. Part of this error may be expected to result from the variation of H$_2$O content with respect to the layer charge (Figure 3a), because the mean H$_2$O coverage values were used. When H$_2$O coverage was plotted as a function of the $CEC/TSSA_{Nr}$ ratio (Figure 6: available from the 'Deposited Material' section of journal pages on The Clay Minerals Society's website: www.clays.org/journal/ JournalDeposits.html) and the resulting regression was used to refine the $TSSA$ calculation, the mean error was reduced to 4% (Table 7). An alternative calculation method directly using $WBW$ and the average $WBW/TSSA_{Nr}$ value as the factor produced similar values and similar errors (Table 7).

The calculations presented above used $TSSA_{Nr}$, *i.e.* they assumed that all smectite surfaces were accessible to H$_2$O. Similar calculations, with similar errors, can be made taking $TSSA_{EXCH}$ as the reference surface.

*TSSA from EGME retention.* The EGME-retention data were first evaluated for the correspondence to the monolayer coverage. The theoretical monolayer retention was calculated for all samples using equation 6, a liquid density of EGME (0.931 g/cm$^3$), and the thickness of EGME monolayer calculated from $d_{001}$ = 1.707 nm provided by Quirk and Murray (1999). The measured EGME-retention data were recalculated to a H$_2$O-free basis, correcting for all H$_2$O held by the smectite at 110ºC. The comparison of such corrected EGME retention with the theoretical values indicated that, on average, coverage was 114% of a monolayer (Table 8). The theoretical monolayer retention was also used in equation 9 to calculate the EGME molecular area ($a_{EGME}$). The average $a_{EGME}$ from this calculation was 0.49 nm$^2$ (Table 8), while equation 8 gave 0.43 nm$^2$. Both calculations were only approximate, because $t$ corresponds to the interlayers containing EGME and H$_2$O (not fully dehydrated clay), but they are reasonably close to the value of 0.4 nm$^2$, established experimentally on alumina reference samples (Chiou *et al.*, 1993). These calculations confirm that EGME retention corresponds reasonably closely to the monolayer coverage to offer a good chance for accurate $TSSA$ measurement.

Table 8 contains the results of the $TSSA_{Nr}$ calculation from the EGME retention. The measured values of mg of EGME/g clay dried at 110ºC were converted into EGME coverage values using the $TSSA_{Nr}$ calculated from the

structural formulae. The dispersion of these EGME coverage values for the investigated set of smectite samples is slightly less than the dispersion of the H$_2$O coverage values. The mean value of 0.39 mg of EGME/m$^2$ clay was used to calculate $TSSA_{Nr}$ and the results compared to the $TSSA_{Nr}$ calculated from the structural formulae. The mean relative error is 5.5% (Table 8), as in the case of H$_2$O-based measurements (Table 7), but the maximum errors are slightly less. Like H$_2$O adsorption, the EGME coverage is correlated with the layer charge, and thus with the $CEC/TSSA_{Nr}$ ratio. Using the latter, poor correlation (Figure 7: available from the 'Deposited Material' section of journal pages on The Clay Minerals Society's website: www.clays.org/ journal/JournalDeposits.html) for the refinement of the $TSSA_{Nr}$, the mean error was reduced to 4.5% (Table 8).

### $Q_s$ from CEC and $TSSA_{H_2O}$ or $TSSA_{EGME}$

The data presented in Table 9 demonstrate that $Q_s$ can be calculated using equation 11 and $TSSA_{EXCH}$ measured by H$_2$O and EGME sorption, with accuracy comparable to the calculation employing the $TSSA_{EXCH}$ from the formula. The mean errors in this calculation are 6% and 5.5%, respectively, and it can be reduced to 4.7% by averaging the results. In order to convert $TSSA_{H_2O}$ and $TSSA_{EGME}$ from Tables 7 and 8, which correspond to $TSSA_{Nr}$, into $TSSA_{EXCH}$ the relevant values were decreased by 4%, based on the average difference between $TSSA_{Nr}$ and $TSSA_{EXCH}$ (Table 1).

### $TSSA_{EXCH}$ and $Q_s$ from CEC and %H$_2$O

Both the $CEC$ and % H$_2$O values are dependent on $Q_s$ and $TSSA$. For $CEC$, this relationship is described by equation 11, which refers to $TSSA_{EXCH}$. Figure 8 (available from the 'Deposited Material' section of journal pages on The Clay Minerals Society's website: www.clays.org/journal/JournalDeposits.html) shows the relationship between the $WBW/TSSA_{EXCH}$ ratio and $Q_s$. From equation 11 and from the regression in Figure 8, both $TSSA_{EXCH}$ and $Q_s$ can be calculated with an average error close to 6% (Table 9). Similar calculations can be performed for EGME.

### *Averaging TSSA from H$_2$O and EGME measurements*

The errors in H$_2$O- and EGME-based measurements of $TSSA$ are random. Thus, averaging the results further reduces the relative error. For unrefined values, where $TSSA$ values are not corrected for the dependence of H$_2$O or EGME coverage on $Q_s$, averaging the % H$_2$O- and % H$_2$O + $CEC$-based calculations reduces the mean error to 5.1%. In this operation, $TSSA_{EXCH}$ obtained from the % H$_2$O + $CEC$-based calculation is converted to $TSSA_{Nr}$ by multiplying by 1.04. This is the average factor based on the data in Table 1. Further error reduction to 4.4% can be obtained by including the EGME-based $TSSA$ in the average. For the refined $TSSA$ values, the error can be reduced to 3.1% (Table 9).

Table 8. Monolayer coverage by EGME, EGME molecular area, and *TSSA* calculations based on EGME absorption. The % error with respect to $TSSA_{Nr}$ values obtained from structural formulae in Table 1 (see text for details).

| Data column | 1 | 2 | 3 | 4 | 5 | 6 | 7 | 8 | 9 | 10 |
|---|---|---|---|---|---|---|---|---|---|---|
| Sample | mg EGME/g smectite (measured) | mg EGME/g smectite (corrected) | Theoretical mono- layer coverage | % monolayer | EGME molecular area | mg EGME/m² | *TSSA* from EGME | % error | *TSSA* from EGME refined | % error |
| Units | mg/g | mg/g | mg/g | % | nm² | mg/m² | m²/g | % | m²/g | % |
| Wyoming | 294 | 293 | 265 | 111 | 0.48 | 0.39 | 748 | −2 | 781 | 3 |
| Mont. #20 | 307 | 309 | 261 | 118 | 0.51 | 0.41 | 781 | 4 | 795 | 6 |
| Chambers | 317 | 318 | 266 | 120 | 0.51 | 0.41 | 805 | 5 | 782 | 2 |
| Texas | 292 | 296 | 266 | 111 | 0.48 | 0.38 | 741 | −3 | 751 | −2 |
| Otay | 327 | 336 | 266 | 126 | 0.54 | 0.43 | 831 | 9 | 804 | 5 |
| Cheto | 301 | 309 | 266 | 116 | 0.50 | 0.39 | 764 | 0 | 739 | −3 |
| Kinney | 324 | 335 | 265 | 127 | 0.55 | 0.43 | 824 | 8 | 801 | 5 |
| Ferr. Sm. | 300 | 306 | 249 | 123 | 0.53 | 0.42 | 763 | 7 | 765 | 7 |
| Garfield | 258 | 261 | 238 | 109 | 0.47 | 0.38 | 656 | −4 | 629 | −8 |
| Uley | 242 | 240 | 244 | 99 | 0.42 | 0.34 | 615 | −12 | 622 | −11 |
| Hectorite | 278 | 279 | 264 | 105 | 0.45 | 0.37 | 708 | −7 | 743 | −2 |
| Saponite | 287 | 290 | 266 | 109 | 0.47 | 0.38 | 730 | −4 | 757 | −1 |
| Mean | 294 | 298 | 260 | 114 | 0.49 | 0.39 | 747 | 5.5 | 747 | 4.5 |

Table 9. Columns 1–8: $Q_s$ from $CEC$ and $TSSA$ based on measured $H_2O$ and EGME retention (equation 11), compared with the value from the two equations approach (see text). The relative errors are calculated with respect to $Q$ values obtained from structural formulae in Table 1. Columns 9–16: $TSSA_{EXCH}$ from the two-equation approach and examples of $TSSA$ error reduction by averaging results from $H_2O$ and EGME-based calculations (from Tables 7, 8, and 9). The relative errors are calculated with respect to $TSSA_{Nr}$ values obtained from structural formulae in Table 1.

| Data column Sample | 1 $Q_s$ from $TSSA_{H_2O}$ | 2 % error | 3 $Q_s$ from $TSSA_{EGME}$ | 4 % error | 5 Mean $Q_s$ | 6 % error | 7 $Q_s$ from two-eq. | 8 % error | 9 $TSSA_{EXCH}$ from two-eq. | 10 % error | 11 Mean $TSSA$ from $H_2O$ | 12 % error | 13 Mean $TSSA$ from EGME and $H_2O$ | 14 % error | 15 Mean $TSSA$ from EGME and $H_2O$ ref. | 16 % error |
|---|---|---|---|---|---|---|---|---|---|---|---|---|---|---|---|---|
| Units |  | % |  | % |  | % |  | % | m²/g | % | m²/g | % | m²/g | % | m²/g | % |
| Wyoming | 0.40 | 11 | 0.35 | −1 | 0.37 | 5 | 0.37 | 0 | 670 | −8 | 682 | −11 | 715 | −6 | 753 | −1 |
| Mont. #20 | 0.40 | 1 | 0.37 | −5 | 0.39 | −2 | 0.38 | −9 | 738 | 4 | 751 | 0 | 766 | 2 | 780 | 4 |
| Chambers | 0.51 | 6 | 0.46 | −4 | 0.49 | 1 | 0.57 | 15 | 622 | −16 | 691 | −10 | 748 | −2 | 734 | −4 |
| Texas | 0.44 | 7 | 0.42 | 1 | 0.43 | 4 | 0.45 | 5 | 660 | −11 | 695 | −9 | 718 | −6 | 731 | −4 |
| Otay | 0.45 | −9 | 0.46 | −6 | 0.46 | −7 | 0.46 | −8 | 791 | 6 | 838 | 10 | 835 | 9 | 808 | 6 |
| Cheto | 0.46 | −1 | 0.49 | 6 | 0.47 | 3 | 0.47 | −3 | 752 | 4 | 799 | 5 | 782 | 2 | 755 | −1 |
| Kinney | 0.45 | −3 | 0.44 | −4 | 0.45 | −4 | 0.46 | −5 | 756 | 3 | 801 | 5 | 812 | 7 | 787 | 3 |
| Ferr. Sm. | 0.44 | −3 | 0.41 | −8 | 0.42 | −5 | 0.44 | −5 | 683 | −2 | 715 | 0 | 739 | 3 | 740 | 3 |
| Garfield | 0.48 | −7 | 0.56 | 8 | 0.52 | 1 | 0.51 | −2 | 680 | 1 | 737 | 8 | 696 | 2 | 666 | −3 |
| Uley | 0.41 | −4 | 0.47 | 9 | 0.44 | 3 | 0.40 | −11 | 681 | 2 | 702 | 0 | 658 | −6 | 667 | −5 |
| Hectorite | 0.35 | 10 | 0.36 | 13 | 0.35 | 12 | 0.31 | −9 | 774 | 9 | 763 | 0 | 736 | −3 | 775 | 2 |
| Saponite | 0.41 | 3 | 0.41 | 2 | 0.41 | 2 | 0.39 | −3 | 715 | −5 | 734 | −4 | 732 | −4 | 768 | 1 |
| Mean | 0.43 | 5.7 | 0.43 | 6.6 | 0.43 | 4.6 | 0.43 | 6.3 | 710 | 5.9 | 742 | 5.1 | 745 | 4.4 | 747 | 3.1 |

## DISCUSSION

### Weight basis of CEC and TSSA measurements

Newman (1987) considered the error problem related to the weight basis for *CEC* measurements. He proposed to solve it by referring to the ignited weight, and demonstrated that for a beidellite, the value of $Q$ calculated from such *CEC* is identical to the $Q$ obtained from the formula. This solution is adequate for mono-mineral samples with known quantities of OH, but cannot be applied to mixtures of clays with different OH content (*e.g.* smectite + kaolinite) and to mixtures of clays with minerals losing other molecules when ignited (*e.g.* smectite + calcite). Kodama and Brydon (1968) proposed the calculation on a 400ºC basis, but this approach is applicable only to low-Fe samples. Our approach has the potential to solve the problem of the weight basis for all chemical compositions and also for mineral mixtures.

### Monolayer H₂O coverage at 47% RH

The total amount of bound $H_2O$ (BW) in Wyoming Ca-montmorillonite at 47% RH measured by TGA-MS, when expressed as moles per *MW* (Table 5) corresponds closely to the value established by Ferrage *et al.* (2005b, their table 2) from detailed profile modeling of XRD patterns. When expressed as mg/g of dry clay (Table 7), *BW* of Wyoming and Cheto Ca-smectite correspond closely to the values measured by Chiou and Rutherford (1997, their figure 1) from vapor-uptake isotherms. The identity of the molecular area of $H_2O$ ($a_{H_2O}$) calculated for Ca-smectite using the interlayer spacing (equation 8) and a two-dimensional, close-packing model (Chiou *et al.*, 1993) is a strong indicator that at 47% RH interlayer

$H_2O$ is indeed arranged mostly as two layers with a density close to 1* and the outer surfaces of the crystals are covered by one $H_2O$ layer, as argued earlier by Newman (1983).

A question may be asked if 47% RH indeed represents the optimum conditions for the development of monolayer water coverage of Ca-smectite surfaces. This problem can be tested by calculating theoretical masses of monolayer $H_2O$ at different RH values using equation 6, and comparing them to the measured water retention values (Table 10). The calculation should comprise low- and high-charge smectite, as the correlation between charge and water retention has been established (Figure 3a). The theoretical mass of $H_2O$ in low-charge (Wyoming) and high-charge (Cheto) Ca-smectite at different RH values was calculated (for liquid water density) from data in Table 1, $t_s = 0.96$ nm, $r = 100$ nm, and $t_w$ based on the formula of Ferrage *et al.* (2005a), which relates the interlayer spacing to RH. The measured masses of $H_2O$ are from the isotherms of Chiou and Rutherford (1997). The measured ranges of RH corresponding to a dominant two-layer $H_2O$ complex with a $d_{001}$ close to 1.5 nm were taken from Sato *et al.* (1992).

Table 10 indicates that high-charge smectite contains more $H_2O$ at a given RH and develops a two-layer complex at lower RH than does low-charge smectite. In both cases, the measured masses of $H_2O$ are smaller than predicted for a two-layer complex at low RH and higher than predicted for a high RH. Table 10 suggests that the best compromise value would be 60% RH, where there is 88% of the theoretical $H_2O$ for the Wyoming smectite and 109% for the Cheto smectite sample. However, the Chiou and Rutherford (1997) isotherms are referenced to

Table 10. Relative humidity effects on theoretical monolayer $H_2O$ content of smectite calculated for *TSSA* = 763 m²/g, liquid water density, and water layer thickness obtained from $d_{001}$, which in turn was calculated from RH using the formula of Ferrage *et al.* (2005a). The theoretical calculation is compared with isothermal measurements of Chiou and Rutherford (1997) for low-charge (Ca-Wyoming) and high-charge (Ca-Cheto) smectite samples. Boxes indicate ranges of two-layer $H_2O$ complexes recorded by Sato *et al.* (1992).

| Data Column RH (%) | 1 $d_{001}$ Ca-Sm nm | 2 H₂O layer thickness nm | 3 Theor. mass of H₂O in smectite mg/g | 4 Meas. mass of H₂O in Wyoming mg/g | 5 % Theor. % | 6 Meas. mass of H₂O in Cheto mg/g | 7 % Theor. % |
|---|---|---|---|---|---|---|---|
| 10 | 1.49 | 0.26 | 201 | | | | |
| 20 | 1.50 | 0.27 | 206 | | | 158 | 77 |
| 30 | 1.51 | 0.28 | 210 | | | 187 | 89 |
| 40 | 1.52 | 0.28 | 215 | 153 | 71 | 207 | 96 |
| 47 | 1.53 | 0.29 | 218 | 170 | 78 | 220 | 101 |
| 50 | 1.53 | 0.29 | 219 | 179 | 82 | 225 | 103 |
| 60 | 1.55 | 0.29 | 224 | 197 | 88 | 245 | 109 |
| 70 | 1.56 | 0.30 | 228 | 214 | 94 | 266 | 117 |
| 80 | 1.57 | 0.31 | 233 | 232 | 100 | 287 | 123 |
| 90 | 1.58 | 0.31 | 237 | 251 | 106 | | |
| 100 | 1.59 | 0.32 | 242 | | | | |

110ºC 'dry mass', and thus the actual $H_2O$ masses should be greater. Our measurements at 47% RH indicate that there is 90% of theoretical $H_2O$ for Wyoming smectite and 104% for Cheto smectite when all $H_2O$ is accounted for (Table 5). At 20% RH, which corresponds to full monolayer coverage according to BET measurements (Quirk and Murray, 1999), low-charge smectite develops mostly one-$H_2O$ interlayer complex while high-charge smectite contains less $H_2O$ than predicted for a two-layer complex (Table 10). Thus, the suggestion of Quirk and Murray (1999) to use 19% RH as standard conditions for the *TSSA* measurements from $H_2O$ content is unfortunate, and 47% RH seems to be the best choice.

### XRD vs. gravimetric data on water content of smectite

Several explanations have been offered in the literature regarding the systematic $H_2O$ mass increase while the two-layer complex remains stable over a range of RH, as shown by XRD measurements of $d_{001}$. The excess $H_2O$ was attributed to unrestricted multi-layer adsorption on external surfaces and capillary condensation (Newman, 1983; Cases *et al.*, 1997; Quirk and Murray, 1999), to layer expansion and capillary condensation (Chiou and Rutherford, 1997), and to clustering of $H_2O$ molecules around exchange cations on the external surfaces (Laird, 1999). On the other hand, it has been well documented recently that capillary condensation becomes a factor only at high RH of 80% and more (Rinnert *et al.*, 2005, and literature cited therein).

The studies of Sato *et al.* (1992) and Ferrage *et al.* (2005a, 2005b) indicate that mixed-layering is a more feasible explanation of the mass increase with RH while XRD data indicate a stable 2-layer $H_2O$ complex. A $d_{001}$ spacing of 1.5 nm indicates that a two-layer $H_2O$ structure is dominant, but does not exclude the coexistence of zero-, one-, and three-layer $H_2O$ structures. Thus, a smaller-than-predicted $H_2O$ content corresponds to an admixture of zero and one-layer $H_2O$ structures (Ferrage *et al.*, 2005a), while greater than predicted $H_2O$ content indicates the development of three-layer structures (table 5 in Sato *et al.*, 1992). The mixed-layer model also explains the greater $H_2O$ content of high-charge compared to low-charge smectite at the same RH (*e.g.* Chiou and Rutherford, 1997, and this paper), as high-charge smectite develops two-layer complexes at lower RH values (data from Sato *et al.*, 1992, presented in boxes in Table 10). The model is also fully consistent with the charge heterogeneity in smectite samples shown by the alkylammonium technique (*e.g.* Mermut and Lagaly, 2001).

### Amount and location of the tightly bound water

Tightly bound $H_2O$ on the surfaces of 2:1 layer clay minerals, which is removable by heating to 400ºC, was observed for sericite by Kodama and Brydon (1968) using a combination of chemical and TGA data. The location of $H_2O$ in the vacant interlayer sites of illite was demonstrated by Slonimskaya *et al.* (1978). A recent study by Drits and McCarty (2007) confirmed this interpretation, and it is also supported by our evaluation of the mass of tightly bound $H_2O$ per *MW* (Table 4). A comparable amount of tightly bound $H_2O$ has been detected on surfaces of trioctahedral vermiculites (Reichenbach and Beyer, 1994).

### Examples of practical applications of this study

Equation 11 allows interpretation of experimental relationships between the *CEC* and *TSSA* of soil and rock samples. For example, a linear relationship of $CEC = 0.223 \times TSSA$ established by Bigorre *et al.* (2000) for some French soils indicates, when analyzed using equation 11, that $Q_s$ is stable at $Q_s = 0.65$ (assuming $d_{06} = 0.15$ nm, a value typical of dioctahedral structures).

Figure 6 demonstrates that the maximum effect of charge density on the $H_2O$ content of natural Ca-smectite samples at 47% RH is ±10%; a result close to those reported by Laird (1999) for Mg-smectite at 54% RH. This finding and the data from Tables 3 and 6 allow for the reinterpretation of the $H_2O$ content *vs.* *CEC* relationship published recently for Ca-bentonites by Kaufhold (2005). The values of *CEC* and $H_2O$ content indicate that the investigated bulk bentonite rocks contain from ~30 to 100% smectite, and that the amount of smectite is the main factor controlling both *CEC* and $H_2O$ values.

The EGME retention values measured in this study (Table 8) cover a similar range to the data reported for smectite by Tiller and Smith (1990). Our conclusions are more optimistic than those of Churchman *et al.* (1991) as we documented that EGME retention can be used for quite precise measurement of the *TSSA* in smectite.

### Smectite b-axis unit-cell parameter and Fe content

Equation 3, derived from our data, is close to the regression of the *b*-axis cell parameter *vs.* (Fe + Mg) established by Desprairies (1983), which was based on a greater number of samples. Adding Mg to our regression does not improve it, and adding the data for trioctahedral smectite makes the regression worse, indicating that in this respect di- and trioctahedral smectites should be treated separately, and Fe should be considered as the controlling factor for the *b*-axis dimension. Köster *et al.* (1999) came to the same conclusion concerning the Fe control on the *b* parameter. Their linear regression, based on five Fe-rich smectites, differs from ours by extrapolating to a smaller *b* parameter for an Fe-free smectite.

## CONCLUSIONS

(1) Ca-smectite, equilibrated at 47% RH contains $16-19$ wt.% $H_2O$ (*BW*), which corresponds closely

(88−107%) to the complete theoretical monolayer coverage of the *TSSA*. Most of the *BW* is released by heating up to 200ºC (*WBW*), but only ~78% of the *BW* leaves Ca-smectite at 110ºC, which is a commonly used dehydration temperature in *CEC* and *TSSA* measurements. A positive correlation between *WBW* and layer charge is observed (Figure 3a), but no correlation with charge location was found (Figure 3b).

(2) An amount of molecular water, on the order of 1% of the air-dried mass of smectite, *i.e.* about half a mole per molecular weight, remains in Ca-smectite even after prolonged heating at 200ºC. The mass of this water (*TBW*) is independent of charge (Figure 4), but it is controlled by the nature of the interlayer cation (Table 4).

(3) If raw *CEC* data determined on a weight basis measured at 110ºC are used to calculate *EXCH* and $Q_s$ (equations 9 and 10, respectively), the resulting values are underestimated with respect to the structural formula data (Figure 5). This underestimation almost disappears if *CEC* values are corrected for $H_2O$ still held by the clay at 110ºC.

(4) EGME retention was evaluated as corresponding to ~114% of the theoretical monolayer coverage. If the average $H_2O$ coverage measured from *WBW*, and EGME coverage obtained in this study for Ca-smectite are used, *TSSA* can be calculated from $H_2O$ and EGME retentions, respectively. The accuracy is similar in the two cases, with the mean error from 5 to 7%, and the maximum error between 12 and 16% (Tables 7 and 8). Averaging the *TSSA* measurements from $H_2O$ and EGME reduces the mean error to 4% and the maximum error to 9%. Errors may be reduced further to ~3% for the mean error and ~6% for the maximum, if a correction for the dependence of $H_2O$ and EGME retention on the layer charge is applied (Figures 7 and 8).

A precise and accurate *TSSA* measurement by a sorption technique is especially important when dealing with multi-phase natural rock samples for which the direct *TSSA* calculation from the chemical formulae of the smectite or I-S is not available.

## REFERENCES

Ammann, L., Bergaya, F., and Lagaly, G. (2005) Determination of the cation exchange capacity of clays with copper complexes revisited. *Clay Minerals*, **40**, 441−453.

Avena, M.J., Valenti, L.E., Pfaffen, V., and De Pauli, C.P. (2001) Methylene blue dimerization does not interfere in surface area measurements of kaolinite and soils. *Clays and Clay Minerals*, **49**, 168−173.

Bardon, C., Bieber, M.T, Cuiec, L., Jacquin, C., Courbot, A., Deneuville, G., Simon, J.M., Voirin, J.M., Espy, M., Nectoux, A., and Pellerin, A. (1983) Recommandations pour la détermination expérérimentale de la capacité d'échange de cations des milieux argileux. *Revue de l' Institut Francais du Pétrole*, **38**, 621−626.

Bergaya, F. and Vayer, M. (1997) CEC of clays: measurement by adsorption of a copper ethylendiamine complex. *Applied Clay Science*, **12**, 275−280.

Bigorre, F., Tessier, D., and Pedro, G. (2000) Contribution des argiles et des matiéres organiques á la rétention de l'eau dans les sols. Signification et role fondamental de la capacité d'échange en cations. *Comptes Rendu Academy of Science Paris, Sciences de la Terre et des planetes*, **330**, 245−250.

Blum, A.E. and Eberl, D.D. (2004) Measurement of clay surface areas by polyvinyl pyrrolidone (PVP) sorption and its use for quantifying illite and smectite abundance. *Clays and Clay Minerals*, **52**, 589−602.

Brindley, G.W. and Brown, G. (1980) *Crystal Structures of Clay Minerals and their X-ray Identification*. Monograph No. **5**, Mineralogical Society, London.

Carter, D.L., Heilman, M.D., and Gonzalez, C.L. (1965) Ethylene glycol monoethyl ether for determining surface area of silicate minerals. *Soil Science*, **100**, 356−360.

Cases, J.M., Berend, I., Francois, M., Uriot, J.P., Michot, L.J., and Thomas, F. (1997) Mechanism of adsorption and desorption of water vapor by homoionic montmorillonite: 3. the $Mg^{2+}$, $Ca^{2+}$, $Sr^{2+}$ and $Ba^{2+}$ exchanged forms. *Clays and Clay Minerals*, **45**, 8−22.

Chabra, R., Pleysier, J., and Cremers, A. (1975) The measurement of cation exchange capacity and exchangeable cations in soils. A new method. *Proceedings of the International Clay Conference*, 1975, Mexico, 439−449.

Chiou, C.T. and Rutherford, D.W. (1997) Effects of exchanged cation and layer charge on the sorption of water and EGME vapors on montmorillonite clays. *Clays and Clay Minerals*, **45**, 867−880.

Chiou, C.T., Rutherford, D.W., and Manes, M. (1993) Sorption of $N_2$ and EGME vapors on some soils, clays, and mineral oxides and determination of sample surface areas by use of sorption data. *Environmental Science & Technology*, **27**, 1587−1594.

Churchman, G.J., Burke, C.M., and Parfitt, R.L. (1991) Comparison of various methods for the determination of specific surfaces of subsoils. *Journal of Soil Science*, **42**, 449−461.

Ciesielski, H. and Steckerman, T. (1997) A comparison between three methods for the determination of cation exchange capacity and exchangeable cations in soils. *Agronomie*, **17**, 9−16.

Desprairies, A. (1983) Relation entre le parametre b des smectites et leur contenu en fer et magnesium. Application a l'etude des sediments. *Clay Minerals*, **18**, 165−175.

Dohrmann, R. and Echle, W. (1994) Eine kritische Betrachtung der Silber-Thioharnstoff-Methode (AgTu) zur Bestimmung der Kationenaustauschkapazitaet und Vorstellung eines neuen methodischen Ansatzes. *Berichte der Deutschen Ton- und Tonmineralgruppe, 3*, 213−222.

Drits, V.A. and McCarty, D.K. (2007) The nature of structure-bonded $H_2O$ in illite and leucophyllite from dehydratation and dehydroxylation experiments. *Clays and Clay Minerals, 55*, 45−58.

Dyal, R.S. and Hendricks, S.B. (1950) Total surface of clays in polar liquids as a characteristic index. *Soil Science*, **69**, 421−432.

Eberl, D.D., Środoń, J., and Northrop, H.R. (1986) Potassium fixation in smectite by wetting and drying. Pp. 296−326 in: *Geochemical Processes at Mineral Surfaces* (J.A. Davis and

K.F. Hayes, editors). ACS Symposium Series **323**, American Chemical Society.

Emmerich, K. and Wolters, F. (2005) The role of crosschecks for the classification of montmorillonite. *Berichte der Deutschen Ton- und Tonmineralgruppe,* **11**, 18−19.

Ferrage, E., Lanson, B, Sakharov, B.A., and Drits, V.A. (2005a) Investigation of smectite hydration properties by modeling experimental X-ray diffraction patterns. Part I. Montmorillonite hydration properties. *American Mineralogist*, **90**, 1358−1374.

Ferrage, E., Lanson, B., Malikova, N., Plançon, A., Sakharov, B.A., and Drits, V.A. (2005b) New insights in the distribution of interlayer $H_2O$ molecules in bi-hydrated smectite from X-ray diffraction profile modeling of 00l reflections. *Chemistry of Materials,* **17**, 3499−3512.

Gates, W.P., Slade, P.G., Manceau, A., and Lanson, B. (2002) Site occupancies by iron in nontronites. *Clays and Clay Minererals*, **50**, 223−239.

Güven, N. (1988) Smectites. Pp. 497−559 in: *Hydrous Phyllosilicates* (S.W. Bailey, editor). Reviews in Mineralogy **19**, Mineralogical Society of America, Washington D.C.

Hendricks, S.B., Nelson, R.A., and Alexander L.T. (1940) Hydration mechanism of the clay mineral montmorillonite saturated with various cations. *Journal of the American Chemical Society,* **62**, 1457−1464.

Jackson, M.L. (1975) *Soil Chemical Analysis − Advanced Course.* Published by the author, Madison, Wisconsin, USA.

Kaufhold, S. (2005) Influence of layer charge density on the determination of the internal surface area of smectites. *Berichte der Deutschen Ton- und Tonmineralgruppe,* **11**, 20−26.

Khoury, H.N. and Eberl, D.D. (1981) Montmorillonite from the Amargosa Desert, southern Nevada, USA. *Neues Jahrbuch für Mineralogie*, **141**, 134−141.

Kodama, H. and Brydon, J.E. (1968) Dehydroxylation of microcrystalline muscovite. *Transactions of the Faraday Society,* **551**, 3112−3119.

Köster, H.M., Erlicher, U., Gilg, H.A., Jordan, R., Murad, E., and Onnich, K. (1999) Mineralogical and chemical characteristics of five nontronites and Fe-rich smectites. *Clay Minerals*, **34**, 579−599.

Lagaly, G. and Weiss, A. (1969) Determination of the layer charge in mica-type layer silicates. *Proceedings of the International Clay Conference*, Tokyo, 61−80.

Laird, D.A. (1999) Layer charge influences on the hydration of expandable 2:1 phyllosilicates. *Clays and Clay Minerals*, **47**, 630−636.

MacEwan, D.M.C. and Wilson, M.J. (1980) Interlayer and intercalation complexes of clay minerals. Pp. 197−248 in: *Crystal Structures of Clay Minerals and their X-ray Identification* (G.W. Brindley and G. Brown, editors). Monograph No. **5**, Mineralogical Society, London.

Meier, L.P. and Kahr, G. (1999) Determination of the cation exchange capacity (CEC) of clay minerals using the complexes of copper(II) ion with triethylenetetramine and tetraethylenepentamine. *Clays and Clay Minerals*, **47**, 386−388.

Mermut, A.R. and Lagaly, G. (2001) Baseline studies of The Clay Minerals Society Source Clays: layer-charge determination and characteristics of those minerals containing 2:1 layers. *Clays and Clay Minerals*, **49**, 393−397.

Michot, L.J. and Villieras, F. (2006) Surface area and porosity.

Pp. 965−978 in: *Handbook of Clay Science* (F. Bergaya, B.K.G. Theng and G. Lagaly, editors). Developments in Clay Science **1**, Elsevier, Amsterdam.

Moore, D.M. and Reynolds, R.C. (1997) *X-ray diffraction and the Identification and Analysis of Clay Minerals.* Oxford University Press, Oxford-New York, 378 pp.

Nadeau, P.H., Wilson, M.J., McHardy, W.J., and Tait, J. (1984) Interstratified clays as fundamental particles. *Science*, **225**, 923−925.

Newman, A.C.D. (1983) The specific surface of soils determined by water sorption. *Journal of Soil Science,* **34**, 23−32.

Newman, A.C.D. (1987) The interaction of water with clay mineral surfaces. Pp. 237−271 in: *Chemistry of Clays and Clay Materials* (A.C.D. Newman, editor). Mineralogical Society Monograph No. **6**, Longman, Essex, UK.

Orsini, L. and Remy, J.-C. (1976) Utilisation du chlorure de cobaltihexammine pour la determination simultanee de la capacite d'echange et des bases echangeables des sols. *Science du Sol,* **4**, 269−275.

Quirk, J.P. and Murray, R.S. (1999) Appraisal of the ethylene glycol monoethyl ether method for measuring hydratable surface area of clays and soils. *Soil Science Society of America Journal*, **63**, 839−849.

Reichenbach, H. Graf v. and Beyer, J. (1994) Dehydration and rehydration of vermiculites: I. Phlogopitic Mg-vermiculite. *Clay Minerals,* **29**, 327−340.

Rinnert, E., Carteret, C., Humbert, B., Fragneto-Cusani, G., Ramsay, J.D.F., Delville, A., Robert, J.-L., Bihannic, I., Pelletier, M., and Michot, L.J. (2005) Hydration of a synthetic clay with tetrahedral charges: a multidisciplinary experimental and numerical study. *Journal of Physical Chemistry B,* **109**, 23745−23759.

Ristori, G.G., Sparvoli, E., Landi, L., and Martelloni, C. (1989) Measurement of specific surface areas of soils by p-nitrophenol adsorption. *Applied Clay Science*, **4**, 521−532.

Sato, T., Watanabe, T., and Otsuka, R. (1992) Effects of layer charge, charge location, and energy change on expansion properties of dioctahedral smectites. *Clays and Clay Minerals*, **40**, 103−113.

Slonimskaya, M.V., Drits, V.A., Finko. V.I., and Salyn, A.L. (1978) The nature of interlayer water in fine-dispersed muscovites. *Izvestiya Akademii Nauk SSSR, seriya geologicheskaya*, **10**, 95−104 (in Russian).

Środoń, J., Elsass, F., McHardy, W.J., and Morgan, D.J. (1992) Chemistry of illite-smectite inferred from TEM measurements of fundamental particles. *Clay Minerals*, **27**, 137−158.

Theng, B.K.G., Ristori, G.G., Santi, C.A., and Percival, H.J. (1999) An improved method for determining the specific surface areas of topsoils with varied organic matter content, texture and clay mineral composition. *European Journal of Soil Science,* **50**, 309−316.

Tiller, K.G. and Smith, L.H. (1990) Limitations of EGME retention to estimate the surface area of soils. *Australian Journal of Soil Research*, **28**, 1−26.

Watanabe, T. and Sato, T. (1988) Expansion characteristics of montmorillonite and saponite under various relative humidity conditions. *Clay Science*, **7**, 129−138.

# LIST OF SYMBOLS

$a_{H_2O}$ ($nm^2$) − the molecular area of $H_2O$, *i.e.* the surface area covered by one $H_2O$ molecule (equations 8 and 9)

Av − coefficient of the Avogadro number (602.2)

$b$ (nm) − $b$ axis unit-cell parameter

*BW* (%) − bound water: experimentally measured wt.% of all water held on clay at 47% RH (equation 7)

*CEC* (meq/100 g) − cation exchange capacity

$d_s$ ($g/cm^3$) − dry (solid) density

$d_w$ ($g/cm^3$) − water density

*EXCH* (charge units/$O_{10}(OH)_2$) − number of exchangeable cations per formula

*FIX* (charge units/$O_{10}(OH)_2$) − number of fixed cations per formula

$f_{SBW}$ − portion of bound water released after heating to 200°C, expressed as a fraction of *WBW* (equation 7)

$H_2O_{mono}$ (%) − theoretical wt.% of monolayer of water on clay surface, calculated using equation 6

$m_{H_2O}$ (mg/g) − $H_2O$ retention in Ca-smectite equilibrated at 47% RH, used in equation 9

*MW* (g/mol) − molecular weight of dry smectite (without molecular water)

$Q$ (charge units/$O_{10}(OH)_2$) − total layer charge (includes exchangeable and fixed cations)

$Q_s$ (charge units/$O_{10}(OH)_2$) − smectitic layer charge (only exchangeable cations)

$r$ (nm) − radius of a fundamental particle of smectite

$t_w$ (nm) − thickness of monolayer of water molecules on smectitic surface

$t_s$ (nm) − thickness of individual silicate layer

$N$ − number of silicate layers in fundamental particle

*TSSA* ($m^2/g$) − general symbol for the total specific surface area of smectite (including interlayers)

$TSSA_{EXCH}$ ($m^2/g$) − total specific surface area corresponding only to exchangeable cations

$TSSA_N$ ($m^2/g$) − total specific surface area calculated excluding crystal edges (equation 4)

$TSSA_{Nr}$ ($m^2/g$) − total specific surface area calculated including crystal edges (equation 1)

*TBW* (%) − experimentally measured wt.% of molecular water held on clay above 200°C

*WBW* (%) − experimentally measured wt.% of water released by clay equilibrated at 47% RH up to 200°C (equation 7)

$\%_{mono}$ (%) − experimentally measured water retention expressed as a percentage of theoretically calculated monolayer coverage (equation 9)

Published online by Cambridge University Press